ELSEVIER

Biochimica et Biophysica Acta 1184 (1994) 178–192

BBA Biochimica et Biophysica Acta

Kinetics of electron transfer and electrochromic change during the redox transitions of the photosynthetic oxygen-evolving complex

Fabrice Rappaport *, Mireille Blanchard-Desce [1], Jérôme Lavergne

Institut de Biologie Physico-Chimique, 13, rue Pierre et Marie Curie, 75005 Paris, France

(Received 6 July 1993)

Abstract

The flash-induced kinetics of formation of the successive S-states of the oxygen-evolving complex were analyzed through absorption changes at 295 nm and in the blue region (440–424 nm). The 295 nm change monitors electron transfer from the charge-storing system towards the oxidized tyrosine Y_Z. The blue absorption changes are due to a local electrochromic shift that was previously shown to vary in size, both in response to electron transfer and to proton release from the catalytic center. The kinetics of proton release can thus be estimated by comparing the 295 nm and electrochromic responses. The half-times found for electron transfer (at pH 6.5) were 250 μs for $Y_Z^+S_0 \rightarrow Y_ZS_1$, 55 μs for $Y_Z^+S_1 \rightarrow Y_ZS_2$, 290 μs for $Y_Z^+S_2 \rightarrow Y_ZS_3$ and 1.2 ms for $Y_Z^+S_3 \rightarrow Y_ZS_0$. The electrochromic kinetics are markedly biphasic during the $Y_Z^+S_3 \rightarrow Y_ZS_0$ transition, with a fast phase ($t_{1/2} \approx 30$ μs) accounting for 40% of the total amplitude and a slow phase ($t_{1/2} \approx 1.2$ ms) concomitant with S_0 and O_2 formation. The fast electrochromic decay is accompanied by a lag in the electron transfer kinetics. This phase is interpreted as reflecting the electrostatically triggered expulsion of one proton from the catalytic center caused by the positive charge on Y_Z^+. This first step then allows the 1.2 ms reaction to take place. The electrochromic kinetics were also found to be globally faster than electron transfer for the $Y_Z^+S_0 \rightarrow Y_ZS_1$ transition above pH 6.5, suggesting similarly a Y_Z^+-induced deprotonation.

Key words: Photosystem II; Oxygen evolving complex; Tyrosine-Z; Proton release; Electrochromism

1. Introduction

Photosynthetic oxygen evolution is driven by the reaction center of Photosystem II (PS II) and catalyzed by the manganese complex on the donor side of the center. The overall reaction, $2H_2O \rightarrow O_2 + 4H^+$, involves four electrons which are abstracted through successive photochemical turnovers of the reaction center. The formal description of the process is given by the Kok cycle [1] defining 5 successive oxidation states (S_0 to S_4) of the oxygen-evolving complex. Each of the $S_i \rightarrow S_{i+1}$ transitions is driven by a single photochemical turnover of PS II. State S_4 spontaneously deactivates towards S_0 in the 1 ms time-range with concomitant liberation of dioxygen. The other higher oxidation states, S_2 and S_3, deactivate slowly (minutes) in the dark towards the stable state S_1. Experimentally, illumination of the system by short saturating flashes is the closest approach to single turnover advancement of the S clock. Progressive scrambling is, however, inevitable during a flash train due to a probability of photochemical misses and, depending on the flash duration, double hits. The chemical nature of the successive S-states has been the object of numerous recent investigations (see review by Debus [2]). While it seems likely that oxidations of Mn atoms are responsible for the two lower oxidation steps, it is debatable whether this also applies to the third step ($S_2 \rightarrow S_3$) for which formation of an oxidized amino acid radical has been alternatively suggested [3,4]. State S_4 does not necessarily require an additional carrier besides tyrosine Y_Z, the intermediate donor transiently involved in the preceding transitions. EPR measurements [5] have estab-

* Corresponding author. Fax: +33 1 40468331.

[1] Present address: Chimie des Interactions Moléculaires, Collège de France, Place Marcelin Berthelot, 75005 Paris, France.

Abbreviations: BBY, granal membrane preparation according to Berthold et al. [27]; DCBQ, 2,6-dichloro-*p*-benzoquinone; DCMU, 3-(3,4-dichlorophenyl)-1,1-dimethylurea; FCCP, carbonylcyanide *p*-trifluoromethoxyphenylhydrazone.

SSDI 0005-2728(93)E0173-N

lished that the 1 ms decay of $Y_Z^+S_3$ is concomitant with the O_2 release reaction [6] or reformation of S_0 [7], so that, at least from a kinetic viewpoint, S_4 is equivalent to $Y_Z^+S_3$.

The process of proton release during the Kok cycle is obviously an important piece of information for understanding the mechanism of photosynthetic water oxidation, since protons are involved as a product of the reaction and also play a major role in the way the system handles the electrostatic constraints implied by accumulation of oxidized species (see [8] for a recent review). It was established by Fowler [9] that the four protons are not all released concomitantly with the oxygen-evolving reaction, but in a more gradual way. The prevailing view for a long period was a stoichiometric pattern 1,0,1,2 for proton release during the successive transitions. Recent work using thylakoids [10,11], or 'BBY' granal membranes [12] showed that this was an oversimplification and that, in fact, the release pattern is generally non-integer and pH-dependent. The Junge group (see [8]) recently reported marked differences for the pH dependence of thylakoids and BBYs. A still different pattern was found in oxygen-evolving PS II core particles [13–15], close to 1,1,1,1. While the significance of the discrepancies between various materials remains to be understood [8], a clear conclusion is that there is no strict stoichiometric coupling of the oxidation and deprotonation steps, but a more flexible interplay between proton releasing groups and charge carriers.

The aim of the present work is to analyze kinetic aspects of electron transfer and proton release during the successive S-transitions. Following the oxidation of the secondary donor, tyrosine Y_Z (in a sub-μs reaction with S-dependent kinetics [16]), the $Y_Z^+S_i \rightarrow Y_ZS_{i+1}$ reactions take place at different rates on each transition (reviewed by Debus [2]). Our goal has been to improve the experimental determination of these kinetics and compare them, at various pHs, with those of proton release. Several possibilities could be envisaged, with different mechanistic implications. A strict coupling of proton release and reduction of Y_Z^+, such as expected for a 'chemical deprotonation' [8,12] would imply concomitant kinetics, while electrostatically induced deprotonation may yield a different picture. The proton release rate may then be faster or slower than electron transfer, depending on the geometry of the system and intrinsic deprotonation rates of the groups involved.

Our first attempt was to measure kinetics of proton release under similar conditions as used in previous work [12] when determining the stoichiometric pattern in BBYs with hydrophilic pH-indicating dyes. This method was, however, unsuccessful, since besides the difficulty of subtracting the uptake kinetics from the acceptor side, the release kinetics were complex with large contribution of slow phases in the 10 ms range. Presumably, the slow response of hydrophilic dyes in this material is due to diffusion barriers between the water oxidation center and the aqueous medium, either reflecting a proteinaceous shield on the donor side of PS II (see [8]), or resulting from the appressed structure of the membrane fragments.

Since our primary concern was to obtain information on the faster events taking place in the vicinity of the catalytic region, we resorted to a different approach (first described in [17]) that takes advantage of an endogenous probe of electrostatic changes occurring on the donor side of PS II. In the regions of the absorption peaks of chlorophyll *a*, the spectral changes associated with the S-transitions have the shape of the first derivative of an absorption band, suggesting an electrochromic shift of such a chlorophyll [4,18] (this *local* effect should not be confused with the electrochromic shift of carotenoids and chlorophylls responding to the *delocalized* membrane potential [24]). In previous work [12] the extent of this shift on each S-transition was analyzed as a function of pH and compared with the titration of the stoichiometric pattern of proton release. Both responses were found to be correlated, within the experimental accuracy, showing that the electrochromic probe senses the balance of electrostatic events in the catalytic center (electron abstraction and proton release).

Since the electrochromic signal reflects the extent of proton release, it can be used as a means for monitoring the kinetics of this release. However, the electrochromic change is also sensitive to the location of the positive charge during the electron transfer reaction between Y_Z and the region of the Mn cluster. Roughly, the presence of one positive charge on Y_Z^+ causes a two-fold larger electrochromic response than when located on the catalytic center [20]. This implies that the probe is closer to Y_Z than to the Mn cluster and agrees with the hypothesis that it could be identified with P680 [25]. Therefore, in order to retrieve the specific information on the kinetics of proton release, we have to take into account the contribution of the $Y_Z^+S_i \rightarrow Y_ZS_{i+1}$ reactions to the electrochromic change.

In order to compare with appropriate accuracy the kinetics of electron transfer and electrochromic response during the $Y_Z^+S_i \rightarrow Y_ZS_{i+1}$ reactions, it seemed preferable to measure both responses under similar conditions, rather than rely on the previously published data for electron transfer. Thus, electron transfer kinetics were obtained from parallel measurements at 295 nm. This approach proved in fact indispensable, since our results show that the fast rate previously estimated for the $Y_Z^+S_0 \rightarrow Y_ZS_1$ reaction (e.g., $t_{1/2} \approx 30$ μs [26]) is largely in error. As our goal was to resolve possibly multiphasic kinetics of the electrochromic change (revealing different time courses for electron

transfer and proton release), particular care had to be taken for retrieving the individual kinetics of each transition from flash sequence data. Previous work either relied on estimates using directly the first flashes of a sequence (in which the dominant transitions are successively $S_1 \rightarrow S_2$, $S_2 \rightarrow S_3$, $S_3 \rightarrow S_4 \rightarrow S_0$, $S_0 \rightarrow S_1$), or on fitting the data by assuming a single exponential for each transition with appropriate weighting computed from the damping parameters. The first method, which neglects the progressive scrambling of the S-transitions, is very inaccurate beyond the second flash, and the second one is not adapted for our purpose since it presupposes that each transition follows simple first-order kinetics. We thus had to resort to an ab initio method, where the experimental sequence of datapoints measured at a given time after the flash is treated independently to obtain the individual contribution of each transition at this particular time. By 'independently', we mean that no kinetic correlation is assumed between different times, while, of course, identical Kok parameters are used in the computation. As may be expected, such a procedure amplifies the scatter of the primary experimental data, and the results presented below have required considerable averaging.

2. Materials and methods

BBY membranes were prepared as described in [27], omitting the second Triton incubation. The membranes were used at a concentration of 10 μg chlorophyll per ml in a medium containing 0.3 M sucrose, 10 mM NaCl and 25 mM buffer (MES in the pH range 6–6.5, Hepes in the pH range 7–7.5). 25 μM 2,6-DCBQ was used as an acceptor. The absorption changes were measured using the Joliot-Béal spectrophotometer [28,29] as previously described [4,12]. This machine uses monochromatic pulses from a xenon flashlamp as a detecting beam. Since the shortest time spacing between successive flashes is about 3 ms, kinetics in the first few ms after an actinic flash were obtained by compiling a number of experiments with different timing of the first detector flash with respect to the actinic pulse. Saturating actinic flashes were provided by a xenon lamp (2 μs duration at half height), filtered by a Schott RG-665 red filter. The detecting photodiode was protected from the actinic light by a blue filter (Corning BG-38), even in the UV region, as explained below.

2.1. UV measurements

The kinetics of the $Y_Z^+ S_i \rightarrow Y_Z S_{i+1}$ reactions were derived from absorption changes at 295 nm. A specific problem was encountered when measuring UV absorption changes in the 200 μs range following a saturating flash. In order to protect the measuring diode from the actinic flash, a UV-transmitting filter has to be used that cuts out actinic light in the visible range. However, the various commercial or home-made filters that we tried allow some transmission in the near infrared, letting through part of the chlorophyll fluorescence pulse excited by the actinic flash. This causes an artefact in the 200 μs range which we could minimize to some extent but not completely suppress. In the preliminary report on this work [17], the artefact had to be measured independently and subtracted, implying a heavier experimental procedure and lower accuracy or possible systematic errors. This problem has now been overcome thanks to an ingenious system designed in the laboratory by D. Béal. A piece of white paper is inserted between the cuvette and a broadband blue filter (Corning BG-38) placed in front of the measuring diode. The 'brighteners' used by manufacturers for improving the 'whiteness' of the paper have a broad absorption in the near UV and high fluorescence yield. The idea is thus to convert the UV light into blue fluorescence. The blue filter transmits this fluorescence but blocks the red light from the actinic flash and the chlorophyll fluorescence. The yield of the system was improved by impregnating the paper with ethylene glycol. Comparing the diode response equipped with our usual UV filter (Corion SB-300) or with Béal's system, the efficiency of the latter is about 50% (at 295 nm) with the gain of total suppression of the artefact problem.

2.2. Deconvolution of the individual contribution of each S-transition

As discussed in detail elsewhere [4,12], three parameters need to be known for retrieving these contributions from flash sequence data, according to Kok's model: the initial distribution of the two dark-stable states (S_0 and S_1), the miss (α) and double-hit (β) probabilities. The damping parameters α and β were determined from the sequence of absorption changes at 295 nm as previously described [4,22]. When initiating this work [17] we used a preillumination by one flash followed by 60 s dark deactivation in the presence of 10 nM FCCP in order to preset the system at $\geq 97\%$ S_1, as described earlier [4,12]. Most of the present experiments were done in a different way, using no preillumination and in the absence of FCCP. The initial distribution of S_1/S_0 was determined from the 295 nm sequence, using previously determined extinction coefficients for the S-transitions. These coefficients were carefully measured at each pH using the methods described in [4], with similar results to those reported in this reference and no significant pH dependence. The initial S_1 concentration thus found routinely in the dark-adapted samples was about 90%. As

indicated in the Introduction, the set of Kok parameters determined in this manner was used for retrieving the contribution of each S-transition to the sequence data-set obtained for each time in the UV and blue regions. As discussed elsewhere [4,19,30], the signal on the first flash contains an additional contribution from inactive centers and was accordingly left out of the deconvolution procedure. The flashing period was 500 ms.

With respect to our previous report [17], the modifications of the experimental procedure consist of: use of 2,6- instead of 2,5-DCBQ; use of Béal's system in the UV; absence of FCCP and preillumination as just described. The only data-set borrowed from [17] is that of Fig. 7.

3. Results

3.1. Kinetics of electron transfer

The time-course of electron transfer between Y_Z and the charge-storing system was recorded at 295 nm. One reason for this choice is that the kinetic interference of the acceptor side is negligible at this wavelength, as will be argued below. In this region, the $Y_Z^+ - Y_Z$ spectrum [18,31–33] corresponds to an absorption increase, which is about half the increase associated with the $S_1 \rightarrow S_2$ transition. From the spectral changes determined for the S-transitions [4], one thus expects the following pattern: an absorption increase on both $Y_Z^+S_1 \rightarrow Y_ZS_2$ and $Y_Z^+S_2 \rightarrow Y_ZS_3$, the latter being smaller than the former, an absorption decrease on $Y_Z^+S_0 \rightarrow Y_ZS_1$ (corresponding to the small UV change found for $S_0 \rightarrow S_1$) and a large decrease for $Y_Z^+S_3 \rightarrow Y_ZS_0$ accompanying the decay of the absorbance built up during the $S_1 \rightarrow S_2$ and $S_2 \rightarrow S_3$ steps.

The deconvoluted kinetics for each transition were plotted in Figs. 1 (pH 6.5) and 2 (pH 7.5). The initial part of the $Y_Z^+S_0 \rightarrow Y_ZS_1$ and $Y_Z^+S_3 \rightarrow Y_ZS_0$ reactions at both pHs was replotted in Fig. 3 on expanded scales. Some preliminary remarks should be made about these results.

A first comment concerns the contribution of acceptor side kinetics at 295 nm. This wavelength is slightly longer than that of the isosbestic point of the $Q_A^- - Q_A$ spectrum (292 nm) so that the initial change includes a small increase due to Q_A^-. What really concerns us, however, is the possible subsequent changes caused at 295 nm by acceptor reactions. These are expected to occur in two different time-ranges. Reoxidation of Q_A^- takes place in the several hundred μs range, as was checked under our conditions by turnover measurements ($t_{1/2} \approx 400$ μs, not shown). When the secondary quinone is initially fully oxidized this results in formation of Q_B^- which in turn disappears with $t_{1/2} \approx 200$ ms (at 25 μM DCBQ), as observed at 325 nm (not shown), giving the quinol form of DCBQ as a final product. As may be seen in the $Y_Z^+S_1 \rightarrow Y_ZS_2$ plot of Fig. 1 and also directly in the first flash trace of Fig. 5, a satisfactory fit is obtained using a single exponential with $t_{1/2} \approx 55$ μs, excluding kinetic contributions in the 400 μs or 200 ms ranges (the open symbol indicates the datapoint at 500 ms). The small overshoot found in [17] does not appear any more. One may conclude that both the $Q_A^-Q_B \rightarrow Q_AQ_B^-$ and $Q_B^- \rightarrow 1/2$ $DCBQH_2$ reactions cause negligible change at 295 nm. Thus, the initial offset caused by Q_A reduction does not vary

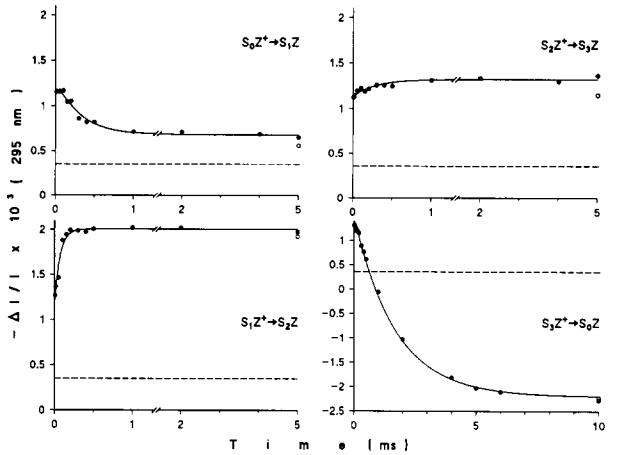

Fig. 1. Kinetics of the $Y_Z^+S_i \rightarrow Y_ZS_{i+1}$ electron transfer reactions at pH 6.5. Individual datapoints were computed from the absorption changes at 295 nm during a flash sequence, as described in the text. The first point was sampled at 6 μs after the actinic flash. The solid curves are fits that take into account both from the 295 nm and electrochromic results (parameters of row C in Table 1, as explained in the Discussion). The open circle in each panel indicate the 500 ms datapoint. The dashed line indicates the average value of this 500 ms level on the four transitions, reflecting the accumulation of reduced acceptor. Notice the different horizontal and vertical scales used for the $Y_Z^+S_3 \rightarrow Y_ZS_0$ kinetics.

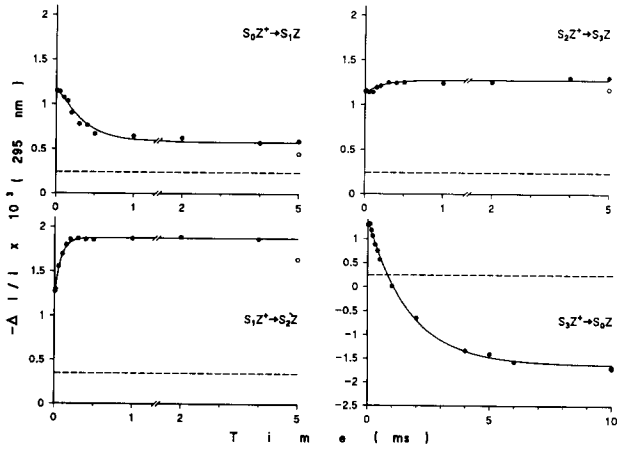

Fig. 2. Kinetics of the $Y_Z^+S_i \rightarrow Y_ZS_{i+1}$ electron transfer reactions at pH 7.5. See legend of Fig. 1.

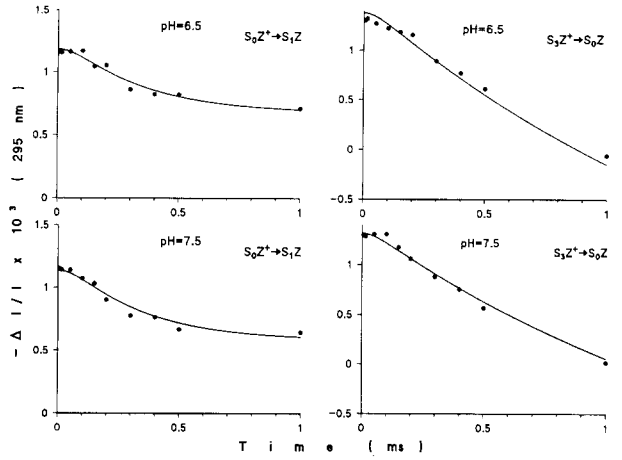

Fig. 3. Kinetics of the $Y_Z^+S_0 \rightarrow Y_ZS_1$ and $Y_Z^+S_3 \rightarrow Y_ZS_0$ electron transfer reactions at pH 6.5 (top) and 7.5 (bottom). Data and fits from Figs. 1 and 2 were replotted on expanded scales.

significantly during subsequent acceptor reactions and may be estimated from the constant offset retrieved from deconvolution of the sequences in the 100–500 ms range (dashed line in Figs. 1, 2). It may be noticed though, that in some of the traces of Figs. 1 and 2, a small decay is observed between 5 and 500 ms for which we have as yet no clear explanation. The final levels (open symbol), when taken with respect to the dashed line, are in good agreement with the previously determined extinction coefficients of the S-transitions at this wavelength [4], although a slightly larger change appears in the present data for $S_0 \rightarrow S_1$. Our discrepancy with previous results from van Gorkom's group on the extent of the UV change on this transition (see [4,19,22,40]) thus becomes narrower (although not insignificant), considering the smaller change now reported by van Leeuwen [39,64].

A second point concerns the initial extent of the signal. Since we are not resolving sub-μs events (the first datapoint lies 6 μs after the actinic flash), the 'initial' amplitude (extrapolated to the time origin) should reflect formation of Y_Z^+ (and a small semiquinone contribution, see above), expected to be constant on each transition. This is not quite true, however, since the signal was consistently found slightly larger on $Y_Z^+S_3$. At pH 6.5, the Y_Z^+ change is about 15% larger on S_3 than on the other states. At pH 7.5, $Y_Z^+S_3$ and $Y_Z^+S_1$ are 10% and 7% larger, respectively, than the two other states. This feature is not due to a deconvolution artefact, since it was also directly apparent to a similar extent on the raw sequence data (not shown). Several explanations can be envisaged. The result obtained at pH 7.5 might suggest a distortion with periodicity of two flashes arising from the acceptor side. These experiments were made in the presence of 25 μM DCBQ, which is not sufficient to allow total reoxidation of the Q_B^- semiquinone in the time interval (500 ms) between flashes. As explained above, a half-time of 200 ms was measured for the semiquinone decay and, accordingly, a small binary oscillation was apparent in the flash sequence at this wavelength (not shown). The reason for using a low DCBQ concentration in these experiments is that elimination of the semiquinone oscillation did not seem necessary for the present purpose, while on the other hand the conditions required for such elimination [4] (150 μM DCBQ, 1 s flash spacing) cause faster degradation of the material and increase the damping. A possible origin of the flash number dependence of the Y_Z^+ signal may thus be the $Q_AQ_B^- \rightleftarrows Q_A^-Q_B$ equilibrium, causing an increased miss probability on even flashes. However, this hypothesis raises several objections. Firstly, the binary semiquinone oscillation has a small extent and rapid damping, since the flash spacing is more than two-fold the half-time of semiquinone decay. Thus a sizeable effect would require an unexpectedly small equilibrium constant for $Q_AQ_B^- \rightleftarrows Q_A^-Q_B$. This is especially unlikely if DCBQ substitutes plastoquinone in the Q_B pocket [4], since a larger equilibrium constant is expected with this high potential quinone. Also, we expect the equilibrium constant to be larger at pH 6.5 than at pH 7.5, which is not consistent with the effect of pH on the absorption change found for $Y_Z^+S_3$. Therefore it is possible that the miss probability depends on flash number for some other reason related to the S-states rather than to the Q_B gate, which would better account for the larger signal found on $Y_Z^+S_3$. We previously reported, however, some evidence obtained in algae against this possibility [4]. Various suggestions of S-dependent misses have been put forward previously [34–39,64], that, unfortunately, would not predict a larger yield of Y_Z^+ upon formation of $Y_Z^+S_3$. Irrespective of the correct interpretation, we checked that the apparent variation of the miss coefficient had no significant consequence on the deconvoluted kinetics presented here: running the computation with the S-dependence of α tailored for restoring a constant initial amplitude of the Y_Z^+ change did not otherwise affect the kinetic features.

The third remark concerns the amplitude of the $Y_Z^+S_2 \rightarrow Y_ZS_3$ kinetics, which is very small in the present results so that the accuracy of the kinetic fit is unwarranted. We have been concerned about the fact that in our earlier experiments [17], which involved a similar amount of signal averaging, a larger amplitude was found for these kinetics. We thus repeated the experiments under the conditions of the previous work and confirmed the small change shown here. However unsatisfactory, this suggests that the spectral changes on the donor side may vary somewhat in different BBY preparations. In spite of the limited accuracy, the kinetic fit obtained on this transition in the present work

is consistent with what we obtained earlier so that we do not consider it as totally unreliable.

The parameters obtained when fitting the results of Figs. 1–3 with simple decay laws were compiled in Table 1 (top). The top row (A) at each pH assumes a mono-exponential time-course and gives the corresponding half-time for the overall kinetics. Whereas this assumption seems valid within experimental accuracy for $Y_Z^+S_1 \rightarrow Y_ZS_2$ and $Y_Z^+S_2 \rightarrow Y_ZS_3$, the two other transitions are better fitted by allowing an initial lag (see Fig. 3). This feature is supported by the finding of biphasic kinetics of the electrochromic signal (described later).

There is a significant discrepancy with previous reports in the half-time of the $Y_Z^+S_0 \rightarrow Y_ZS_1$ reaction. This was considered to be the fastest of the S-state transitions ($t_{1/2} \approx 30$–50 μs, [26,41,42]), whereas we consistently find 215–250 μs. Since the present results derive from a somewhat involved deconvolution procedure, we felt the need for direct cross-checks.

It should be emphasized that, since the first flash is not used in the deconvolution procedure, the loss of

Table 1
Kinetic parameters obtained when fitting the electron transfer (top panel) and electrochromic (bottom panel) kinetics

pH	Fit	Half-times of 295 nm absorption changes			
		$Y_Z^+S_0 \rightarrow Y_ZS_1$	$Y_Z^+S_1 \rightarrow Y_ZS_2$	$Y_Z^+S_2 \rightarrow Y_ZS_3$	$Y_Z^+S_3 \rightarrow Y_ZS_0$
6.5	A	$t_{1/2} = 250$ μs S.D. = 130	$t_{1/2} = 50$ μs S.D. = 100	$t_{1/2} = 290$ μs S.D. = 100	$t_{1/2} = 1.2$ ms S.D. = 196
	C	$t_{1/2} = 50$ μs $t_{1/2} = 210$ μs S.D. = 100	$t_{1/2} = 55$ μs S.D. = 104	$t_{1/2} = 200$ μs S.D. = 104	$t_{1/2} = 30$ μs $t_{1/2} = 1.2$ ms S.D. = 100
7.5	A	$t_{1/2} = 215$ μs S.D. = 126	$t_{1/2} = 50$ μs S.D. = 100	$t_{1/2} = 240$ μs S.D. = 100	$t_{1/2} = 1.2$ ms S.D. = 139
	C	$t_{1/2} = 50$ μs $t_{1/2} = 210$ μs S.D. = 100	$t_{1/2} = 55$ μs S.D. = 109	$t_{1/2} = 150$ μs S.D. = 110	$t_{1/2} = 30$ μs $t_{1/2} = 1.2$ ms S.D. = 100
pH	Fit	Half-times of (440–424 nm) absorption changes			
		$Y_Z^+S_0 \rightarrow Y_ZS_1$	$Y_Z^+S_1 \rightarrow Y_ZS_2$	$Y_Z^+S_1 \rightarrow Y_ZS_2$	$Y_Z^+S_3 \rightarrow Y_ZS_0$
6.5	A	$t_{1/2} = 225$ μs S.D. = 100	$t_{1/2} = 55$ μs	$t_{1/2} = 200$ μs	$t_{1/2} = 840$ μs S.D. = 273
	B	(same as A)	(same as A)	(same as A)	$t_{1/2} = 30$ μs 35% $t_{1/2} = 1.2$ ms 65% S.D. = 100
	C	$t_{1/2} = 50$ μs 2% $t_{1/2} = 210$ μs 98% S.D. = 104	(same as A)	(same as A)	(same as B)
7.0	A	$t_{1/2} = 170$ μs S.D. = 128	$t_{1/2} = 60$ μs	$t_{1/2} = 175$ μs	$t_{1/2} = 760$ μs S.D. = 270
	B	$t_{1/2} = 50$ μs 32% $t_{1/2} = 210$ μs 68% S.D. = 100	(same as A)	(same as A)	$t_{1/2} = 25$ μs 30% $t_{1/2} = 1.2$ ms 70% S.D. = 100
7.5	A	$t_{1/2} = 90$ μs S.D. = 128	$t_{1/2} = 55$ μs	$t_{1/2} = 150$ μs	$t_{1/2} = 610$ μs S.D. = 213
	B	$t_{1/2} = 500$ μs 65% $t_{1/2} = 340$ μs 35% S.D. = 100	(same as A)	(same as A)	$t_{1/2} = 25$ μs 45% $t_{1/2} = 1.1$ ms 55% S.D. = 100
	C	$t_{1/2} = 50$ μs 60% $t_{1/2} = 210$ μs 40% S.D. = 106	(same as A)	(same as A)	$t_{1/2} = 30$ μs 43% $t_{1/2} = 1.2$ ms 57% S.D. = 102

Rows A in both panels indicate the half-times of the monoexponential function that fits best the individual data. Rows B (bottom panel) indicate the half-times for a bi-exponential decay, whenever it resulted in significant improvement of the fit of the elctrochromic kinetics (i.e., for $Y_Z^+S_0 \rightarrow Y_ZS_1$ and $Y_Z^+S_3 \rightarrow Y_ZS_0$). Rows C (both panels) indicate the best compromise found when imposing common rate constants in the 295 nm and electrochromic kinetics. A single exponential was used for transitions $Y_Z^+S_1 \rightarrow Y_ZS_2$ and $Y_Z^+S_2 \rightarrow Y_ZS_3$. For the two other transitions a biexponential decay $A_1 \exp(-k_1t) + A_2 \exp(-k_2t)$ was used for the electrochromic kinetics and a sigmoidal function $A_0/(k_1 - k_2)[k_1 \exp(-k_2t) - k_2 \exp(-k_1t)]$ for the electron transfer kinetics. The quantity S.D. gives for each experimental kinetics a rating of the fits with respect to the best row, computed from the standard deviation between datapoints and theoretical curve: the higher the S.D. in excess of 100, the worse the fit. For the electrochromic kinetics, the best fit (S.D. = 100) is that of row B (or A when B is the same as A); the increase of S.D. in row C is the price paid for having common rate constants with the 295 nm kinetics. For the electron transfer data, row A is the best one for the monoexponential kinetics of the second and third column, whereas for the two other transitions the best fit is obtained in row C that takes into account the lag phase.

information caused by sequence damping is expected to be worst for $S_1 \rightarrow S_2$, which has its major specific contribution only on the fifth flash. Therefore, a direct measurement of the kinetics on this transition should test the quality of the deconvolution in a rather demanding way. The experiment shown in Fig. 4 was done under repetitive conditions in the presence of DCMU, inhibiting electron transfer from Q_A^- to the secondary quinone, so that the flash-induced signal should reflect formation of $S_2Q_A^-$ (which subsequently back-reacts towards S_1Q_A in the seconds range). The repetitive flash illumination (at 20-s intervals) eliminated any contribution from centers initially in S_0. As may be seen, the direct kinetics obtained in this experiment are in very good agreement with the results derived from deconvolution of the $Y_Z^+S_1 \rightarrow Y_ZS_2$ kinetics. This also confirms that the latter did not include significant distortion from acceptor side reactions. Another conclusion is that the contribution of inactive centers in the experiment of Fig. 4 does not appear as a distinct kinetic phase, in agreement with previous findings [4,30] showing that these centers undergo a normal $S_1 \rightarrow S_2$ transition.

A second test consisted of analyzing the kinetics recorded on the first flash in a sample preilluminated either by one flash or by a group of three flashes. This was done conveniently by submitting the sample to a repetitive illumination cycle: 1 flash, 60 s darkness, 3 flashes, 60 s darkness. 10 nM FCCP was added in this experiment in order to ensure complete deactivation of the S_2 and S_3 states during the 60 s dark period. Under such conditions, the sample preilluminated by one flash is almost entirely in the S_1 state, whereas the three flash preillumination leads to a majority of S_0. The one-preflash trace (Fig. 5, circles) confirms the conclusions drawn from the DCMU experiment of Fig. 4: the kinetics are fitted by a single exponential with $t_{1/2} = 55$ μs, identical to the deconvolution result for $Y_Z^+S_1 \rightarrow Y_ZS_2$, and again no specific distortion (besides the amplitude increase) is caused by inactive centers. The kinetics measured after three preillumination flashes (Fig. 5, squares) is expected to combine kinetics from centers initially in S_0 and in S_1, the latter including the contribution of inactive centers. Accordingly, this curve is biphasic with a fast rise corresponding to $Y_Z^+S_1 \rightarrow Y_ZS_2$ and a slower decay due to $Y_Z^+S_0 \rightarrow Y_ZS_1$.The agreement with the deconvoluted results can be shown in a more quantitative way. We may write:

$$C_{1F}(t) = C_1(t) + C_{in}(t)$$

$$C_{3F}(t) = (1-\sigma)C_1(t) + \sigma C_0(t) + C_{in}(t)$$

where C_{1F} and C_{3F} denote the experimental traces after one or three preillumination flashes, C_1, C_0 the kinetics of centers initially in S_1 and S_0, and C_{in} the kinetics of inactive centers. This description assumes that after one preflash, all the active centers are in S_1 and after three flashes a fraction σ is in S_0 (thus, $1-\sigma$ in S_1). Another straightforward assumption (especially taking into account the cyclic experimental procedure) is an identical contribution of inactive centers in both cases. Then the difference between both traces just

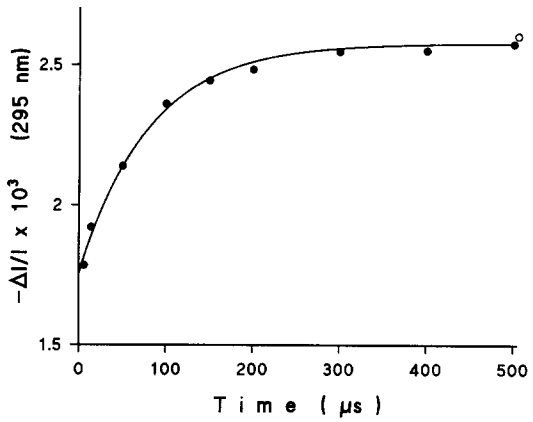

Fig. 4. Kinetics of the flash-induced absorption change at 295 nm in the presence of 25 μM DCMU at pH 6.5. The samples were submitted to 6 illumination cycles (one flash followed by 20 s darkness). The data were averaged over five cycles, discarding the first flash. The open circle is the 100 ms datapoint. The curve is a fit using a single exponential with the 55 μs half-time estimated for the $Y_Z^+S_1 \rightarrow Y_ZS_2$ kinetics computed from flash sequences (Fig. 1).

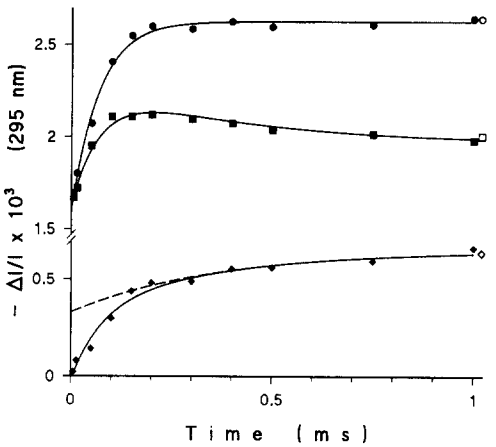

Fig. 5. Kinetics of the flash-induced absorption changes at 295 nm after different preillumination procedures at pH 6.5. The samples (with 10 nM FCCP present), were submitted to 6 illumination cycles (1 flash, 60 s darkness, 3 flashes with 500 ms spacing, 60 s darkness), discarding the first cycle when averaging the data. The top trace (circles) is the kinetics obtained after one preflash (recorded on the first flash in the group of three), the middle trace (squares) correspond to three preflashes (recorded on the single flash). The bottom trace (diamonds) is the difference between the preceding kinetics (one preflash minus three preflashes). The open symbols indicate the 500 ms datapoint. The fits (solid lines) were obtained using the same kinetic parameters as in Fig. 1 (row C in Table 1), assuming 100% and 43% S_1 for, respectively, the top and middle traces (see text). The bottom curve was fitted with the difference $C_1(t) - C_0(t)$ as explained in the text (the dashed line indicates the $C_0(t)$ contribution).

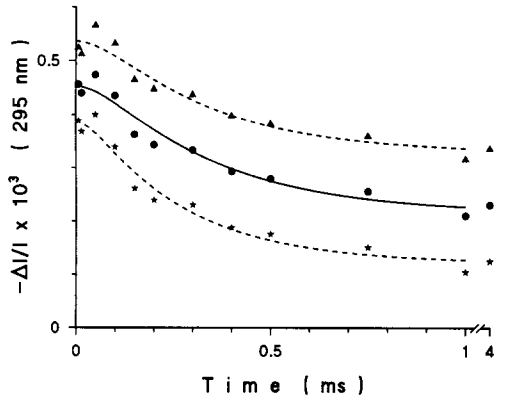

Fig. 6. Estimates of the $Y_Z^+ S_0 \rightarrow Y_Z S_1$ kinetics obtained by subtracting various fractions of the one preflash kinetics from the three preflashes kinetics of Fig. 5. The weighting coefficient was 0.60 (triangles), 0.65 (circles) and 0.70 (stars), corresponding to $\gamma = 0.5$ and, respectively, $\sigma = 0.60$, 0.53 and 0.45 (see text). The fitting curves use the sigmoidal function given in the Discussion; for the middle trace, the kinetic parameters are those estimated for $C_0(t)$ ($Y_Z^+ S_3 \rightarrow Y_Z S_0$ in Table 1, row C), as used in Figs. 1 and 5.

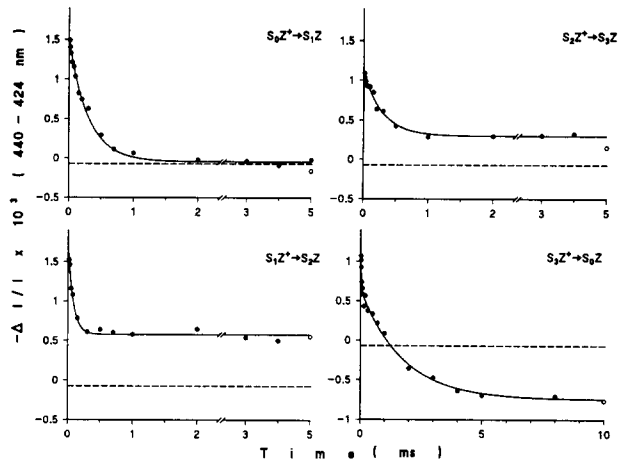

Fig. 7. Kinetics of the electrochromic absorption change (440–424 nm) during each of the $Y_Z^+ S_i \rightarrow Y_Z S_{i+1}$ transitions at pH 6.5. Same conventions as in Figs. 1–2. The fits used single exponentials for $Y_Z^+ S_1 \rightarrow Y_Z S_2$ and $Y_Z^+ S_2 \rightarrow Y_3 S_2$ and a sum of two exponentials for the other transitions, with parameters indicated in Table 1 (bottom panel, row C).

gives $\sigma\ (C_1(t) - C_0(t))$. This difference is the lower plot (diamonds) shown in Fig. 5. The fit shown by the solid line uses $C_1(t) - C_0(t)$ as obtained from deconvolution (Fig. 1). This shows that the direct difference of the 1F and 3F traces is in nice agreement with the kinetics expected from sequence deconvolution. We can go one step further by recalling that the kinetics of inactive centers, $C_{in}(t)$ appear identical to $C_1(t)$. Thus we may write $C_{in}(t) = \gamma C_1(t)$, where γ stands for the amount of inactive centers relative to active ones. Inserting this into the above system yields:

$$\sigma C_0(t) = C_{3F}(t) - (1 - \sigma/(1+\gamma))C_{1F}(t)$$

In other words, the $C_0(t)$ kinetics can be obtained (to within a multiplicative factor) by subtracting from C_{3F} some fraction of C_{1F}. It is of interest to examine the family of curves obtained in this way when varying the subtracted fraction of C_{1F} within a reasonable range, as shown in Fig. 6. Coefficient γ can be estimated from the ratio $(1 + \gamma)$ of the initial signal (due to Y_Z^+ and the Q_A^- contribution) on the first and second (or subsequent) flashes of a sequence, which gives $\gamma \approx 0.50$ in this sample. The fraction σ of S_0 centers in the 3F experiment was estimated to about 53% from analysis of the sequences ('difference method' described in [4]). The middle plot in Fig. 6 was computed using the above parameters, while the top and bottom plots assumed, repectively, $\sigma = 60\%$ or 45%. As may be seen, the middle trace is in good agreement with the kinetic parameters estimated from deconvolution of the $Y_Z^+ S_0 \rightarrow Y_Z S_1$ transition, including the lag phase. From a more qualitative viewpoint, the results of Figs. 5 and 6 show that the estimate of a $t_{1/2}$ in the few hundred μs range for $Y_Z^+ S_0 \rightarrow Y_Z S_1$ is a robust result that does not depend crucially on the precise values estimated for σ or γ.

3.2. Kinetics of the electrochromic response

In order to measure this signal we used the difference of absorption changes between 440 nm and 424 nm (rather than 428 nm as in [12]). The $Q_A^- - Q_A$ spectrum presents equal changes at these wavelengths so that its contribution cancels out in the difference. Also, when examining the results of Figs. 7 and 8 (e.g., for $S_1 \rightarrow S_2$) it appears that further reactions on the acceptor side (400 μs and 200 ms ranges, as explained above) have negligible contribution. The results obtained at pH 6.5 are shown in Fig. 7, those at pH 7.5 in Fig. 8. The initial part of the $Y_Z^+ S_0 \rightarrow Y_Z S_1$ and $Y_Z^+ S_3$

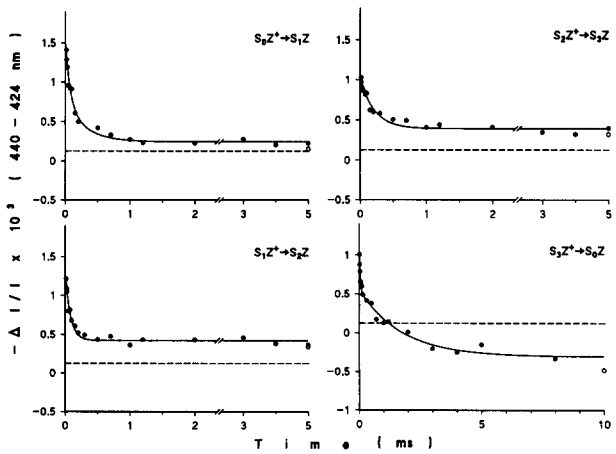

Fig. 8. Kinetics of the electrochromic absorption change (440–424 nm) during each of the $Y_Z^+ S_i \rightarrow Y_Z S_{i+1}$ transitions at pH 7.5. See legend of Fig. 7.

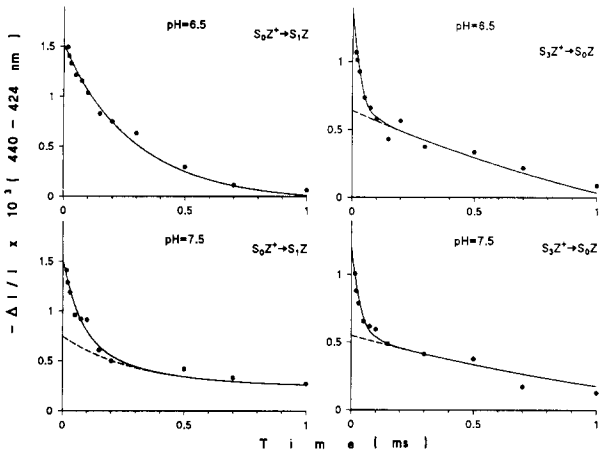

Fig. 9. Kinetics of the electrochromic absorption change during the $Y_{Z+}S_0 \rightarrow Y_ZS_1$ and $Y_{Z+}S_3 \rightarrow Y_ZS_0$ transitions at pH 6.5 (top) and 7.5 (bottom). Data replotted from Figs. 7–8 on expanded scales. The dashed lines indicate the extrapolation of the slow phases of the fits.

$\rightarrow Y_ZS_0$ kinetics were replotted on expanded scales in Fig. 9.

The values obtained in the 500 ms range (open symbols in Figs. 7 and 8) may be compared with the pH titration of similar measurements reported in Fig. 6 of [12]. For this comparison, the levels should be referenced to the dashed line indicating the small constant offset occurring on each flash, and the different wavelengths pairs used in [12] should also be taken into account. Qualitatively, similar trends are confirmed for the pH dependence: from pH 6.5 to 7.5, the (440–424 nm) signal increases for $S_0 \rightarrow S_1$, decreases for $S_1 \rightarrow S_2$ and remains about constant for $S_2 \rightarrow S_3$. Nevertheless the pH effect on $S_0 \rightarrow S_1$ appears smaller than expected from our previous work and the level at pH 6.5 is less markedly negative than reported in our previous spectra [4]. We cannot exclude that this discrepancy may arise from different BBY preparations. If, on the other hand, the problem arises from experimental inaccuracy, preference should be given to the present results that have involved more extensive averaging of primary experimental input.

In agreement with the 295 nm results, a satisfactory fit was obtained by assuming a mono-exponential time-course for $Y_Z^+S_1 \rightarrow Y_ZS_2$ and $Y_Z^+S_2 \rightarrow Y_ZS_3$, with similar half-times as in the UV (55 μs for the former and 200 μs or 150 μs for the latter at, respectively, pH 6.5 or 7.5). On the other hand, the kinetics for $Y_Z^+S_0 \rightarrow Y_ZS_1$ at pH 7.5 and $Y_Z^+S_3 \rightarrow Y_ZS_0$ (at both pHs) appear markedly biphasic and have been satisfactorily fitted as a sum of two exponentials. Table 1 (bottom panel) summarizes the kinetic parameters obtained when fitting the results of Figs. 7 and 8 and those (not shown) measured at pH 7.0.

4. Discussion

4.1. Overall rates of electron transfer

The determination of the rates for each of the $Y_Z^+S_i \rightarrow Y_ZS_{i+1}$ reactions was addressed by several techniques in the past literature: turnover measurements of the S-transitions [7,36], EPR measurements of Y_Z^+ [5–44] and absorption changes [20,26,39,41,42,45, 46]. Previously reported values for half-times of these reactions range as follows: < 3 μs [39,46] to 30–70 μs [26,41,42,47] for $Y_Z^+S_0 \rightarrow Y_ZS_1$; 30–40 μs [20,42], 70 μs [45] to 100–140 μs [26,41,44,47] for $Y_Z^+S_1 \rightarrow Y_ZS_2$; 100 μs [42], 220–350 μs [26,41,44,47] to 600 μs [43] for $Y_Z^+S_2 \rightarrow Y_ZS_3$; 1.0–1.5 ms [5,26,41–47] for $Y_Z^+S_3 \rightarrow Y_ZS_0$. The present work yields the following values: 200–250 μs for $Y_Z^+S_0 \rightarrow Y_ZS_1$, 55 μs for $Y_Z^+S_1 \rightarrow Y_ZS_2$, 250–300 μs for $Y_Z^+S_2 \rightarrow Y_ZS_3$, 1.2 ms for $Y_Z^+S_3 \rightarrow Y_ZS_0$.

A novel feature in the present approach has been to compute individually, for each kinetic datapoint, the contribution of the successive S-transitions. This procedure is more demanding on the quality of the experimental input than the methods used previously. The major discrepancy between these results and those compiled above concerns the $Y_Z^+S_0 \rightarrow Y_ZS_1$ reaction. Confronted with the unexpected finding of a much slower rate for this reaction than reported by other authors, we took special care to check the validity of our deconvolution procedure and also seeked a more direct way to estimate the rate of this particular transition. For an overall check of the deconvolution results, we measured the $Y_Z^+S_1 \rightarrow Y_ZS_2$ kinetics either in the presence of DCMU (using a repetitive illumination that excludes centers initially in S_0) or in samples fully deactivated after one preflash (so that the fraction of S_1 is close to 100%). Both results were in very good agreement with the 55 μs kinetics computed from flash sequences. Since this transition is the most difficult to resolve when the first flash is left out of the computation, this provides strong support for the reliability of the deconvoluted results. Concerning the $Y_Z^+S_0 \rightarrow Y_ZS_1$ reaction, a direct way to estimate its time-course is to compare the kinetics following the first flash on a sample with a majority of S_0 (as obtained by preillumination with three flashes) or essentially in S_1 (one preflash). This approach (Figs. 5 and 6) gave a clear confirmation of the kinetic features derived from deconvolution of the flash sequence data. As to the contradiction with previous results, we put forward the following remarks. Firstly, it is quite difficult to estimate the kinetic contribution of the $Y_Z^+S_0 \rightarrow Y_ZS_1$ transition from flash sequence data without a rigorous deconvolution procedure, since this reaction only appears to a significant extent on the fourth flash, mixed with the preceding ($Y_Z^+S_3 \rightarrow Y_ZS_0$) and subsequent

($Y_Z^+S_1 \rightarrow Y_ZS_2$) transitions. This applies in particular to the EPR data (e.g., [5,43,44]), where the use of highly concentrated samples (hence the difficulty of ensuring sufficiently homogeneous actinic illumination) and absence of independent calibration of the Kok parameters cause significant uncertainty. Taken together with the signal-to-noise ratio and kinetic resolution of these experiments, it seems clear to us that the data reported in these papers are not sharply irreconcilable with our findings. Nevertheless, one may consider an interesting alternative possibility that was suggested to us by one reviewer: the EPR detectability of the tyrosine radical could be specifically decreased in the S_0 state, e.g., through magnetic interaction with the Mn cluster.

Concerning the absorption change experiments, we believe that the major problem arises from the choice of wavelengths (350–360 nm region) at which the previous work was done [26,39,41,42,46,47]. There is no significant absorption change of $Y_Z^+ - Y_Z$ in this region [18,31–33]. However, according to our results [4,22], there is no significant change associated with $S_0 \rightarrow S_1$ either, so that we do not expect a detectable signal for $Y_Z^+S_0 \rightarrow Y_ZS_1$. The finding of a 30–50 μs kinetics may then arise from the contribution of $Y_Z^+S_1 \rightarrow Y_ZS_2$ on the fourth flash caused by double-hits. In recent experiments from van Leeuwen [39,46,64] using PS II core particles, several conclusions from Dekker's work were revised. First, it was recognized that the UV change associated with $S_0 \rightarrow S_1$ was markedly smaller than that associated with the other transitions (although not as small as concluded in our work). Therefore van Leeuwen acknowledged that little signal was expected at 350 nm for $Y_Z^+S_0 \rightarrow Y_ZS_1$ (the same conclusion had been reached by Saygin and Witt [42] and Renger and Hanssum [47]). In spite of this difficulty, these authors attempted to measure these kinetics and concluded that it was limited by the apparatus response, i.e., < 3 μs (it should be noted that no contribution of $S_1 \rightarrow S_2$ occurs on the fourth flash in van Leeuwen's experiments using a short laser flash that causes no double-hitting). We believe that, in fact, the kinetics could not be resolved because of its vanishingly small amplitude rather than a short lifetime. Interestingly, from electroluminescence experiments, Vos and coworkers [48] had earlier found a 300 μs phase for $Y_Z^+S_0 \rightarrow Y_ZS_1$, similar to our estimate, but the authors were reluctant to reject Dekker's estimate on this basis.

4.2. Interpretation of the electrochromic kinetics

The electrochromic response appears sensitive to both the location and magnitude of the positive charge residing on the PS II donor side. The amplitude of the change is decreased about two-fold when the positive charge is transferred from Y_Z to the Mn cluster, as may be seen, e.g., on the $Y_Z^+S_1 \rightarrow Y_ZS_2$ transition at pH 6.5 (Fig. 7), where little proton release occurs. On the other hand, the final magnitude of the net charge depends on the extent of proton release. In previous work [12], we showed that the extent of the electrochromic shift measured at long times after each flash was linearly correlated, within experimental accuracy, with the extent of proton release. If we denote by p_i (pH) the amount of protons released on the ith transition, the electrochromic signal varies as $A_i + B(1 - p_i)$, where A_i and B do not depend on pH. The offset A_i depends on the wavelengths used and may arise mainly from the background spectra of the S-transitions (e.g., tails of the UV bands). The quantity $(1 - p_i)$ is the net electrostatic balance resulting from the abstraction of one electron and release of p_i protons. Coefficient B, that reflects the sensitivity of the probe to the net charge of the catalytic center, was found roughly constant on all transitions (see Fig. 6 in [12]). These studies led us to two conclusions: (i) the electrochromic probe responds to the net charge, irrespective of the precise location of the various charged groups, implying that the scale of these details is small compared with the distance between the catalytic center and the probe; (ii) the net charge change is satisfactorily accounted for by the balance of only electrons and protons, which seems to preclude significant release or uptake of other ions (e.g., Ca^{2+} or Cl^-) during the S-transitions.

Due to its electrostatic origin, the signal should respond instantaneously to electron and proton movements. Thus, whenever the release is not concomitant with the electron transfer reaction, this should appear as a specific kinetic phase of the electrochromic change. We assume for simplicity, but acknowledge this is unwarranted, the absence of transient interference from other possible sources of electrostatic variations than electron transfer and proton release, such as internal displacement of protons or other ions.

There is, however, a complicating feature that appears when considering the initial extent of the electrochromic change after a flash. This should reflect the extent of Y_Z^+, expected to be approximately constant on each transition. However, in agreement with earlier work [20,56], the initial amplitude of the absorption changes used for monitoring the electrochromic signal was found markedly modulated by the S-states (see Figs. 7–9). This may be observed directly on the datapoints measured in the 10 μs range after the flash or by extrapolating the kinetics towards the time origin. This modulation is much larger than that observed for the initial 295 nm change (discussed earlier). Its flash number dependence is also quite different. At pH 6.5 (Fig. 7), the initial (440–424 nm) extent is about 35% larger in states $Y_Z^+S_0$ and $Y_Z^+S_1$ than in states $Y_Z^+S_2$ or $Y_Z^+S_3$. Thus, the more positive the net charge on the

catalytic center, the smaller the initial change at this pair of wavelengths. From previous data obtained in algae [56], and from current investigation (to be reported elsewhere), it appears that the S-dependent modulation of the signal is in fact due to a variable contribution of the $P680^+$-P680 difference spectrum, indicating that a small fraction of $P680^+$ is present in equilibrium with $Y_Z^+S_2$ and $Y_Z^+S_3$. Our interpretation is that the net charge of the catalytic center modulates the Y_Z $P680^+ \rightleftarrows Y_Z^+$ P680 equilibrium. This is in agreement with the finding by Schlodder and coworkers [57] of an S-dependent extent of $P680^+$ in the μs-range that was similarly ascribed to an electrostatic effect. It also accounts for the modulation of the fluorescence yield (since $P680^+$ is known to be a quenching state) reported by Delosme [58]. Whereas the spectral contribution of $P680^+$ distorts the amplitude of the (440–424 nm) changes, it is not expected to affect qualitatively the present interpretations of the kinetics, since this phenomenon, as well as the electrochromic change, reflects electrostatic interactions. This view will be documented in a forthcoming paper.

4.3. Comparison of electron transfer and electrochromic kinetics

The kinetic parameters obtained when fitting both sets of data have been compiled in Table 1, in which the rows presented at each pH correspond to different constraints imposed in the fitting procedure. The top row (A) is the fit obtained with a single exponential. In row (B) of the bottom panel, the electrochromic kinetics were fitted with a sum of two exponentials, whenever this improved the fit. This was the case for $Y_Z^+S_0 \rightarrow Y_ZS_1$ at pH 7.0 and 7.5 and $Y_Z^+S_3 \rightarrow Y_ZS_0$ at all pHs. The quantity denoted S.D. is the standard deviation between the fitting function and the datapoints, normalized at 100 for the best fit: it gives a quantitative rating of the improvement brought about by the two-exponentials fit.

On the two transitions where the electrochromic response is biphasic ($Y_Z^+S_0 \rightarrow Y_ZS_1$ and $Y_Z^+S_3 \rightarrow Y_ZS_0$), the 295 nm kinetics, although acceptably fittable by a single exponential, consistently show a significant initial lag phase (see Fig. 3). This lag occurs in the same time-range as the fast component of the electrochromic decay. There is also a reasonably good agreement between the subsequent electron transfer kinetics and the slow phase of the electrochromic response. In order to account for this, we assumed the following model. On these transitions the global $Y_Z^+S_i \rightarrow Y_ZS_{i+1}$ process consists of two phases: (i) $Y_Z^+S_i \rightarrow (Y_Z^+\ S_i)'$ with rate constant k_1, and (ii) $(Y_Z^+S_i)' \rightarrow Y_ZS_{i+1}$ with rate constant k_2. Step (i) involves an electrostatic relaxation (presumably proton release) monitored through the electrochromic change, but no electron transfer (no UV change). The electron transfer step (ii) should appear in both responses, since the electrochromic signal decreases when the positive charge moves from Y_Z to the Mn region. This model imposes that the 295 nm kinetics has the form: $A_0/(k_1 - k_2)[k_1 \exp(-k_2t) - k_2 \exp(-k_1t)]$, thus entirely determined by the two rate constants and the initial amplitude A_0. The results shown in row (C) of the table were obtained by simultaneously fitting the two indicators, using the above function for the 295 nm change and a bi-exponential decay $(A_1 \exp(-k_1t) + A_2 \exp(-k_2t))$ for the electrochromic kinetics, with the same values of k_1 and k_2 as in the 295 nm kinetics. For the other transitions, that appear monophasic within experimental accuracy, row (C) gives the best compromise obtained when imposing a common rate for both responses.

The only marked effect of pH on the kinetic parameters is the acceleration of the electrochromic decay of $Y_Z^+S_0 \rightarrow Y_ZS_1$ at pH 7.5 (overall half-time ≈ 90 μs) with respect to 6.5 (225 μs), whereas the 295 nm kinetics appears pH independent. A slight acceleration of the $Y_Z^+S_2 \rightarrow Y_ZS_3$ kinetics with pH is also observed. The rates of the two phases of $Y_Z^+S_3 \rightarrow Y_ZS_0$ do not depend significantly on pH, but the relative weight of the fast phase in the electrochromic kinetics seems to increase somewhat at pH 7.5.

4.4. Mechanistic implications

From the foregoing, the $S_1 \rightarrow S_2$ and $S_2 \rightarrow S_3$ transitions appear kinetically simple, while more complexity is involved in the two other transitions. We now address the implications of the kinetics at each S-transition.

The $S_1 \rightarrow S_2$ transition. The $Y_Z^+S_1 \rightarrow Y_ZS_2$ kinetics are seen as a single exponential with $t_{1/2} \approx 55$ μs, both through UV and electrochromic changes and at all pHs investigated. Since there is almost no proton release on this transition at pH 6.5 [12], we did expect identical kinetics for both indicators at this pH. At pH 7.5, however, where about half a proton is released, a different result could, but did not, arise. This suggests that the proton release rate is not limiting i.e., that the k_{off} rate constant is fast compared with the 55 μs electron transfer reaction. This point is not straightforward, however, since the pH dependence of the release on this state has led us to involve a group with a pK of 8.2 in the presence of S_1 shifted to 7.25 in the presence of S_2 [12]. On the other hand, the release rate k_{off} of a protonatable group is related to its binding rate k_{on} and dissociation constant K through: $k_{off} = K\ k_{on}$. Thus, taking a pK of 7.25 and $k_{on} \leq$ the diffusion-limited rate constant (about 10^{11} s^{-1} M^{-1}), one expects $k_{off} \leq 5600$ s^{-1} or $t_{1/2} \geq 120$ μs, which does not meet our requirement. There are, however, several

possibilities allowing a protein-bound group to have a larger effective k_{on} than the diffusion-limited value. If we assume, for example, that a group has a pK of 6 in bulk water and $k_{off} = 10^{11}\ 10^{-6} = 10^5\ s^{-1}$ (or $t_{1/2} = 7$ μs), then placing this group at the surface of a membrane with a local surface potential of, say, −60 mV, will shift its pK to 7 but not affect its k_{off} (in fact the effective k_{on} is increased ten-fold because of the local proton concentration). This type of effect has been proposed by Maroti [49] to account for the observation of proton binding to the acceptor side of bacterial reaction centers at a rate faster than expected for diffusion-limited kinetics. Another possibility of increasing k_{on} is the channelling of protons through hydrogen-bound water molecules (see [50]).

The $S_2 \rightarrow S_3$ transition. This step is accompanied by the release of one proton in the whole pH range 5.5 to 8 [12]. Due to its small amplitude at 295 nm, the electron transfer kinetics is not accurately resolved in the present work (whereas larger changes were obtained, for unclear reasons, in [17]). In this previous work, the electrochromic kinetics were found somewhat faster than electron transfer ($t_{1/2}$ of, respectively, 230 and 310 μs), suggesting that proton release is initiated at the Y_Z^+ stage. A similar trend appears in the present results (see rows (A) in Table 1) but their limited accuracy does not allow a meaningful confirmation.

The $S_3 \rightarrow S_0$ transition. The results obtained for the $Y_Z^+S_3 \rightarrow Y_ZS_0$ reaction are in very good agreement with the two-step model outlined above. The biphasic character of the electrochromic decay is easily discernible in Figs. 7–9, with a fast 30 μs phase accounting for about 40% of the total amplitude and a 1.2 ms phase also observed for the electron transfer kinetics. The 295 nm change displays a lag in the 30 μs time range, during the rapid decay phase of the electrochromic shift. This finding confirms a previous report by Koike and Renger [52] who resolved a lag on the third flash of a sequence, using thermophilic algae with kinetics slowed down at room temperature. The simplest explanation is that the electrostatic constraint resulting from the formation of state $Y_Z^+S_3$ causes the expulsion of a proton from the catalytic center with a release half-time of 30 μs. This electrostatic relaxation decreases the redox potential of the catalytic center, allowing reduction of Y_Z^+ (1.2 ms reaction) to take place. The reason for implying deprotonation of a group closer to the catalytic center than to Y_Z is that otherwise, the electrostatic relaxation would *stabilize* Y_Z^+ rather than trigger its reduction.

It is possible to give a rough approximation of the amount of proton release required to account for the 30 μs decay phase of the electrochromic change. From the $Y_Z^+S_1 \rightarrow Y_ZS_2$ kinetics at pH 6.5 (where no proton is released) it appears that the electrochromic response

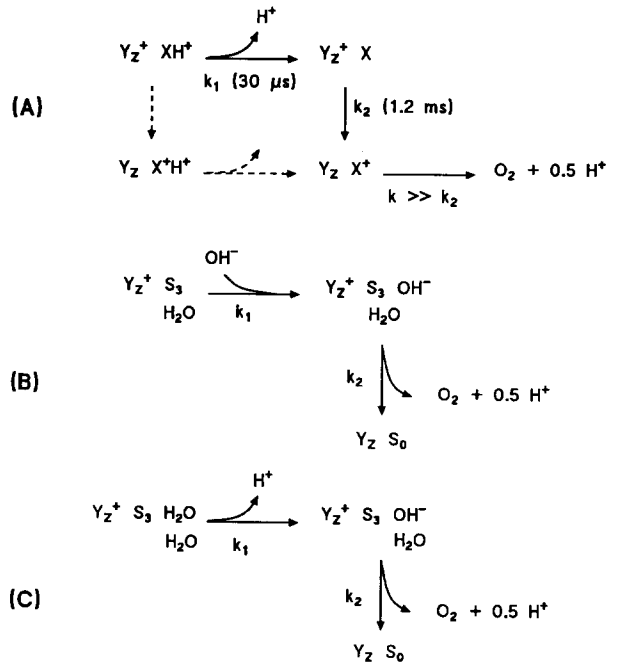

Fig. 10. Possible reaction schemes for $Y_Z^+S_3 \rightarrow Y_ZS_0$. The dashed arrows (omitted for simplicity in B and C) indicate a kinetically unfavourable path. The H^+ release or OH^- binding reaction (rate constant k_1) affects the electrochromic response but causes no absorption change at 295 nm. The electron transfer reaction (rate constant k_2) is observed as a decay in both signals. Scheme A assumes an intermediate carrier X which participates in the concerted oxidation of water. This implies that the latter reaction (rate constant k) is not rate-limiting. In B and C, Y_Z^+ participates directly in water oxidation. The presence of Y_Z^+ induces the binding or OH^- in B, or deprotonation of previously bound water in C. The rate of the first reaction in B is expected to increase ten-fold per pH unit, whereas it is expected to be independent of pH in C.

decays by a factor of about two when the positive charge migrates from Y_Z^+ to the Mn region. A similar extent (about half the initial amplitude) is observed at both pHs for the 30 μs phase of the $Y_Z^+S_3 \rightarrow Y_ZS_0$ kinetics, thus equivalent to a decrease by about one unit of the net charge in the Mn region. This suggests that on the global release of 1.5 protons during this transition [12], about 1 is expelled during the 30 μs phase electrostatically triggered by Y_Z^+.

The reaction schemes shown in Fig. 10 propose several possibilities for this model. Scheme (A) involves a carrier X (e.g., a Mn) that is transiently oxidized by Y_Z^+ in the 1 ms reaction and then reacts with water together with the previously accumulated oxidants. An unappealing feature in this scheme is that water oxidation is not the rate-limiting process, which is rather unlikely considering the activation energy required for this reaction as estimated by Krishtalik [52,53]. In fact, this author emphasized the difficulty of designing a reaction scheme that would lower enough the activation energy to allow *as fast a rate* as experimentally observed (1 ms). We thus propose that Y_Z^+ could be

directly involved in the concerted oxidation of water, as in schemes (B) and (C). These schemes also follow Krishtalik's view that binding the water substrate as OH^-, rather than H_2O, would be very helpful for lowering the activation energy of the water oxidation reaction (see also [54]). Thus, in (B) the rapid electrochromic decay is attributed to OH^- binding instead of H^+ release. However, the rate of this phase was found to be independent of pH, which is not easily accommodated by this hypothesis. Therefore, a more satisfactory possibility is that of scheme (C) which involves proton release from pre-bound water. The involvement of OH^- as a product of the first reaction in schemes (B) and (C) is an independent assumption that is not required by the kinetic scheme: alternatively, the fast proton release may arise from a group that is not a direct substrate.

After the initial rapid expulsion of one proton, the remaining 0.5 proton of the release does not appear as a kinetically distinct phase from the 1.2 ms electron transfer reaction. One actually expects that this release reflects the balance between a larger release resulting from water oxidation and *rebinding* to the groups that deprotonated in the S_0 to S_3 steps. Thus, besides the fast release phase, both the subsequent release and rebinding processes appear to take place concomitantly with the electron transfer reaction. A biphasic time-course of proton release had been previously observed by Förster and Junge [55] on the third flash of a sequence, but the fast component had been attributed to contamination by $S_2 \rightarrow S_3$. However, in recent work from this group (see [8]) a biphasic time course has been resolved for proton release on the $Y_Z^+S_3 \rightarrow Y_ZS_0$ transition in thylakoids (using neutral red), in agreement with our finding. Interestingly, the slower ms-phase may consist of a release, as in our case, or an *uptake* at low pH, where these authors found for this transition a global proton stoichiometry smaller than one.

The $S_0 \rightarrow S_1$ transition. The results obtained at pH 7.5 for the $Y_Z^+S_0 \rightarrow Y_ZS_1$ reaction may suggest, at first sight, a similar mechanism as for $Y_Z^+S_3 \rightarrow Y_ZS_0$. The overall electrochromic kinetics are significantly faster than electron transfer and may be decomposed in two phases. The slower one approximately matches the electron transfer kinetics. Also, a lag phase is resolved in the 295 nm kinetics. This would agree, again, with a Y_Z^+-triggered deprotonation facilitating the electron transfer reaction. We have, however, a number of difficulties with this interpretation. A first problem is that the kinetic fitting using our model is not excellent (e.g., the lifetime of the slow phase at pH 7.5 may be somewhat longer at 295 nm than for the electrochromic change, see Figs. 3 and 9). Although this difficulty with rates may well be within the accuracy range of these data, there is also a problem with the relative amplitude of the slow phase (left-bottom panel in Fig. 9) which is smaller than expected (40% instead of $\geq 50\%$) if it reflects simply the charge displacement on the electron transfer step. The most serious difficulty, however, is to account for the effect of pH that was observed. At pH 6.5 the lag seems to be present to the same extent in the 295 nm kinetics, but the electrochromic response has become essentially monophasic (hence the insignificant 2% amplitude found when imposing a 50 μs fast phase in the fitting procedure). The electrochromic data at pH 7.0 (Table 1) are consistent with the other pHs, showing an intermediate amplitude and similar rate of the fast phase. In our previous work [12], we estimated for this transition a release close to 1 H^+ at pH 7.5 and about 1.25 H^+ at pH 6.5. Thus, we expected a more homogeneous situation at pH 7.5, where all centers give off one proton, than at 6.5 where a fraction of them (25%) give off an additional proton. The actual result is just the opposite; similar kinetics in the two spectral regions were observed at pH 6.5 and a more complex pattern appeared at 7.5. We thus believe that the $Y_Z^+S_0 \rightarrow Y_ZS_1$ process is not adequately described by the two-step mechanism used for $Y_Z^+S_3 \rightarrow Y_ZS_0$, although we are presently unable to propose an explanatory model that would not appear as wild speculation.

Leaving aside possibly misleading kinetic decompositions, the basic information is the following: the electron transfer rate does not depend appreciably on pH; the overall electrochromic kinetics is accelerated when increasing the pH, so that above pH 6.5 it is faster than electron transfer. Therefore, conservative inferences are that: (i) above pH 6.5, an electrostatic relaxation is triggered by Y_Z^+ (H^+ release, OH^- uptake or other); (ii) the acceleration with pH could be indicative of OH^- binding.

Y_Z^+-induced deprotonation. We have been led to involve proton release triggered by the presence of the positive charge on Y_Z^+ in two cases: on the $Y_Z^+S_3$ state, irrespectively of the pH, and on the $Y_Z^+S_0$ state above pH 6.5. Conversely, in the other states (including $Y_Z^+S_0$ at pH 6.5) our results suggest that this process does not occur (except perhaps for $Y_Z^+S_2$) and that proton release accompanies the reduction of Y_Z^+. The occurrence of a deprotonation step triggered by Y_Z^+ does not necessarily imply that the releasing group has to be closer to the tyrosine than to the Mn cluster, since it is clear from the behavior of the electrochromic signal and from the modulation of the rate of electron transfer and equilibrium constant between Y_Z and P680 that the whole donor side of PS II experiences significant mutual electrostatic interactions. On the other hand, a direct deprotonation of the oxidized tyrosine appears very likely considering the low pK of phenoxy-cation radicals. This is expected to take place concomitantly with Y_Z oxidation in the sub-μs range

(below the time resolution of our experiments) and to reverse during the reduction reaction. If such a deprotonation/reprotonation occurs on each turnover, the question arises, how far apart does this proton move? If it were leaving the vicinity of the Y_Z region and expelled to the aqueous medium, this should neutralize the local charge change and cancel the electrochromic effect. Conversely, the reduction-reprotonation of Y_Z^+ should not be detected as an electrochromic change. Therefore, we believe that the deprotonation of Y_Z upon its oxidation involves only a local proton transfer rather than *release* in the sense used here. This is in line with the model proposed by Eckert and Renger [59] or Babcock et al [60] in which a very limited movement of the proton occurs towards a H-bonding ligand of the tyrosine. If this view is correct, there would still be a positive charge present in the immediate environment of the tyrosine radical and our notation for Y_Z/Y_Z^+ stands short for $(Y_ZH...B)/(Y_Z^{\cdot}$ $BH^+)$. Following the formation of the latter species and on a longer timescale, proton release proper may occur, either directly from group B, or from other groups sensing the positive charge of BH^+, depending on electrostatic distances, pK's and kinetic accessibility of proton acceptors or water. In the case of the 30 μs deprotonation phase on $Y_Z^+S_3$, we favor the indirect process involving proton release from the catalytic center, for several reasons: (i) It accounts better for the amplitude of the electrochromic phase that should be larger if the proton was released from $(Y_Z^{\cdot}$ $BH^+)$. (ii) It accounts better for the lag phase in the tyrosine reduction. (iii) It accommodates more easily the possibility that this step may play a useful role for lowering the activation energy of the water oxidation reaction (as, e.g., in schemes B and C of Fig. 10) rather than being a pure waste of oxidizing power.

Two more remarks may be added on this issue. Y_Z^+-induced deprotonation has been observed in Tris-washed material in which the Mn cluster is destroyed [61–63]. This provides no direct indication as to the location of the proton releasing group, although the finding of a relatively high pK (≈ 5) for this process [61] makes it unlikely that the direct deprotonation of tyrosine is involved. This suggests that, even in this damaged system, proton draining from the immediate vicinity of Y_Z is hindered. The second remark concerns the finding by Haumann and Junge (see [8]) that, at variance with our conclusions, a fast release phase can be observed on *all* transitions. In these experiments, using the neutral red technique, the rate of this phase was found to increase linearly with the dye concentration. At the higher concentration used, the rate was in the 10 μs range, with no indication of a saturation. A possible interpretation is that neutral red interferes with the endogenous proton release process by allowing rapid draining of protons from the vicinity of Y_Z^+.

5. Acknowledgements

The skillful technical assistance of Daniel Béal, particularly in designing the UV-blue conversion system, is gratefully acknowledged. The authors wish to thank Dr. David Kramer for discussions and reading the manuscript. Some valuable suggestions from the reviewers have been incorporated in the text. This work was supported by the C.N.R.S.

6. References

[1] Kok, B., Forbush, B. and McGloin, M. (1970) Photochem. Photobiol. 11, 457–475.
[2] Debus, R. (1992) Biochim. Biophys. Acta 1102, 269–352.
[3] Boussac, A., Zimmermann, J.-L., Rutherford, A.W. and Lavergne, J. (1991) Nature 347, 303–306.
[4] Lavergne, J. (1991) Biochim. Biophys. Acta 1060, 175–188.
[5] Babcock, G.T., Blankenship, R.E. and Sauer, K. (1976) FEBS Lett. 61, 286–289.
[6] Joliot, P., Hofnung, M. and Chabaud, R. (1966) J. Chim. Phys. 10, 1423–1441.
[7] Bouges-Bocquet, B. (1973) Biochim. Biophys. Acta 292, 772–785.
[8] Lavergne, J. and Junge, W. (1993) Photosynth. Res. (in press)
[9] Fowler, C.F. (1977) Biochim. Biophys. Acta 462, 414–421.
[10] Lavergne, J. and Rappaport, F. (1990) in Current Research in Photosynthesis (Baltscheffsky, M., ed.), Vol. 1, pp. 873–876, Kluwer, Dordrecht.
[11] Jahns, P., Lavergne, J., Rappaport, F. and Junge, W. (1991) Biochim. Biophys. Acta 1057, 313–319.
[12] Rappaport, F. and Lavergne, J. (1991) Biochemistry 30, 10004–10012.
[13] Wacker, U., Haag, E. and Renger, G. (1990) in Current Research in Photosynthesis (Baltscheffsky, M., ed.), Vol. 1, pp. 869–872, Kluwer, Dordrecht.
[14] Lübbers, K. and Junge, W. (1990) in Current Research in Photosynthesis (Baltscheffsky, M., ed.), Vol. 1, pp. 877–880, Kluwer, Dordrecht.
[15] Van Leeuwen, P.J. (1993) Ph.D. dissertation, Leyden.
[16] Brettel, K., Schlodder, E. and Witt, H.T. (1984) Biochim. Biophys. Acta 766, 403–415.
[17] Lavergne, J., Blanchard-Desce, M. and Rappaport, F. (1992) In Research in Photosynthesis (Murata, N., ed.), Vol. II, pp. 273–280.
[18] Dekker, J.P., Van Gorkom, H.J., Brok, M. and Ouwehand, L. (1984) Biochim. Biophys. Acta 764, 301–309.
[19] Dekker, J.P., Van Gorkom, H.J., Wensink, J. and Ouwehand, L. (1984) Biochim. Biophys. Acta 767, 1–9.
[20] Lavergne, J. (1984) FEBS Lett. 173, 9–14.
[21] Saygin O. and Witt, H.T. (1985) FEBS Lett. 187, 224–226.
[22] Lavergne, J. (1987) Biochim. Biophys. Acta 894, 91–107.
[23] Velthuys, B.R. (1988) Biochim. Biophys. Acta 933, 249–257.
[24] Junge, W. and Witt, H.T. (1968) Z. Naturforsch. 23b 244–254.
[25] Schatz, G. and Van Gorkom, H.J. (1985) Biochim. Biophys. Acta 810, 283–294.
[26] Dekker, J.P., Plijter, J.J., Ouwehand, L. and Van Gorkom, H.J. (1984) Biochim. Biophys. Acta 767, 176–179.
[27] Berthold, D.A., Babcock, G.T. and Yocum, C.F. (1981) FEBS Lett. 134, 231–234.
[28] Joliot, P., Béal, D. and Frilley, B. (1980) J. Chim. Phys. 77, 209–216.
[29] Joliot, P. and Joliot, A. (1984) Biochim. Biophys. Acta 765, 210–218.

[30] Lavergne, J. and Leci, L. (1993) Photosynth. Res. 35, 323–343.
[31] Diner, B.A. and de Vitry, C. (1984) In Advances in Photosynthesis Research (Sybesma, C., ed.), Vol. I, pp. 407–411, Martinus Nijhoff/Dr. W. Junk, The Hague.
[32] Weiss, W. and Renger, G. (1984) FEBS Lett. 169, 219–223.
[33] Gerken, S., Brettel, K., Schlodder, E. and Witt, H.T. (1988) FEBS Lett. 237, 69–75.
[34] Delrieu, M.-J. (1974) Photochem. Photobiol. 20, 441–454.
[35] Delrieu, M.-J. and Rosengard, F. (1991) Biochim. Biophys. Acta 1057, 78–88.
[36] Bouges-Bocquet, B. (1980) Biochim. Biophys. Acta 594, 85–103.
[37] Renger, G. and Hanssum, B. (1988) Photosynth. Res. 16, 243–259.
[38] Shinkarev, V. and Wraight, C.A. (1993) Proc. Natl. Acad. Sci. USA 90, 1834–1838.
[39] Van Leeuwen, P.J., Heimann, C. and Van Gorkom, H.J. (1993) Photosynth. Res. in press.
[40] Dekker, J.P. (1992) in Manganese Redox Enzymes (Pecoraro, V.L., ed.), pp. 85–103, VCH, New York.
[41] Renger, G. and Weiss, W. (1986) Biochim. Biophys. Acta 850, 184–196.
[42] Saygin, Ö and Witt, H.T. (1987) Biochim. Biophys. Acta 893, 452–469.
[43] Cole, J. and Sauer, K. (1987) Biochim. Biophys. Acta 891, 40–48.
[44] Hoganson, C.W. and Babcock, G.T. (1988) Biochemistry 27, 5848–5855.
[45] Velthuys, B.R. (1981) in Photosynthesis (Akoyunoglou, G., ed.), Vol. II, pp. 75–85, Balaban Int. Science Services, Philadelphia.
[46] Van Leeuwen, P.J., Heimann, C., Gast, P., Dekker, J.P. and Van Gorkom, H.J. (1993) Photosynth. Res., in press.
[47] Renger, G. and Hanssum, B. (1992) FEBS Lett. 299, 28–32.
[48] Vos, M.H., Van Gorkom, H.J. and Van Leeuwen, P.J. (1991) Biochim. Biophys. Acta 1056, 27–29.
[49] Maroti, P. (1993) Photosynth. Res. 37, 1–17.
[50] Grunwald, E. (1965) Prog. Phys. Org. Chem. 3, 317–358.
[51] Koike, H., Hanssum, B., Inoue, Y. and Renger, G. (1987) Biochim. Biophys. Acta 893, 524–533.
[52] Krishtalik, L.I. (1986) Biochim. Biophys. Acta 849, 162–171.
[53] Krishtalik, L.I. (1990) Bioelectrochem. Bioenerg. 23, 249–263.
[54] Brudvig, G.W. and De Paula, J.C. (1987) in Prog. Photosynth. Res. (Biggins, J., ed.), pp. 491–498, Nijhoff, Dordrecht.
[55] Förster, V. and Junge, W. (1985) Photochem. Photobiol. 41, 183–190.
[56] Lavergne, J. (1985) Physiol. Vég. 23, 411–423.
[57] Schlodder, E., Brettel, K. and Witt, H.T. (1985) Biochim. Biophys. Acta 808, 123–131.
[58] Delosme, R. (1971) in Proc. IInd Int. Cong. Photosynth. (Forti, G., Avron, M. and Melandri, A., eds.), pp. 187–195, Junk, The Hague.
[59] Eckert, H.-J. and Renger, G. (1988) FEBS Lett. 236, 425–431.
[60] Babcock, G.T., Barry, B.A., Debus, R.J., Hoganson, C.W., Atamian, M., McIntosh, L., Sithole, I. and Yocum, C.F. (1989) Biochemistry 28, 9557–9565.
[61] Förster, V. and Junge, W. (1984) In Advances in Photosynthesis Research (Sybesma, C., ed.) Vol. II, pp. 305–308, Martinus Nijhoff/Dr. W. Junk, The Hague.
[62] Renger, G. and Völker, M. (1982) FEBS Lett. 149, 203–207.
[63] Conjeaud, H. and Mathis, P. (1986) Biophys. J. 49, 1215–1221.
[64] Van Leeuwen, P.J., Heimann, C., Dekker, J.P., Gast, P. and Van Gorkom, H.J. (1992) In Research in Photosynthesis (Murata, N., ed.), Vol. II, pp. 325–328.